Hindawi
Geofluids
Volume 2022, Article ID 3314911, 7 pages
https://doi.org/10.1155/2022/3314911

Research Article

Research on the Ability of Geodetic Records to Explain the Slip Distribution of Wenchuan, China, Earthquake

Yin Deyu

Faculty of Architecture and Civil Engineering, Huaiyin Institute of Technology, Jiangsu, Huai'an 223001, China

Correspondence should be addressed to Yin Deyu; yindeyuiem@163.com

Received 18 March 2022; Revised 12 July 2022; Accepted 17 August 2022; Published 4 November 2022

Academic Editor: Umberta Tinivella

We establish a reasonable 3D complex fault model. The Global Positioning System (GPS) data is adopted to reproduce the slip distribution of the 2008 M_w7.9 Wenchuan earthquake. Utilizing the nonnegative least square method, the slip distribution of the fault plane is recovered. The results are as follows: (1) The released seismic moment of Wenchuan earthquake is 0.959×10^{21} N · m. The deep of the rupture is mainly within 15 km. (2) The rupture mainly occurred along the Beichuan fault, indicating that the Beichuan fault is the main rupture fault. On the southern section of the Beichuan fault, the rupture is concentrated from Yingxiu to Longmenshan and from Yuejiashan to Qingping areas, with mainly thrust slip. On the northern section of the Beichuan fault, the slip is concentrated near the surface of Beichuan and Nanba areas, with thrust and strike slip. On the Pengguan fault, the slip is mainly located near Hanwang with thrust and strike slip. (3) The GPS data are useful for defining the slip in the shallow part but are useless to determine the slip in the deep part. Meanwhile, the time information of the rupture cannot be reproduced.

1. Introduction

The 2008 M_w7.9 Wenchuan earthquake caused a large number of casualties and property losses in China, producing an extremely complex fault along Longmen Shan. The Longmen Shan fault zone where the seismogenic fault is located is of a complex structure, mainly composed of four reverse faults [1]. The earthquake produced a 300 km fault plane; two faults Beichuan Yingxiu fault (Beichuan fault) and Guanxian Jiangyou fault (PengGuan fault) close to parallel in space are formed [2, 3]. The two main rupture zones have surface fractures in the Beichuan Yingxiu fault (BCF) and Pengguan fault (PGF). The former is 240 km long, while the latter is 72 km long [1, 3, 4]. The complex fault and surface rupture show that the rupture process of the Wenchuan earthquake is very complex. Abundant observation records have been obtained after the earthquake, including seismic records, geodetic data (GPS data), and interferometric synthetic aperture radar (InSAR). After the Wenchuan earthquake, abundant research results were obtained. There are very few examples of such rich research results before the Wenchuan earthquake.

For this earthquake, a great deal of researchers have given the rupture history [2, 5–17, 20–23]. These studies give the main characteristics of the rupture: the Wenchuan earthquake is mainly characterized by thrust slip. The length of the fault plane is about 300 km. The rupture duration is about 100 s. The distribution of the slip on the fault plane is very uneven, and the two areas with the largest slip are located in the Yingxiu and Beichuan areas with the most serious earthquake damage.

The role of GPS data in source rupture inversion is a research hotspot. In the existing studies using GPS data, the south section of BCF mostly adopts a single dip model. This is different from the real situation. The dip angle of the southern segment of BCF increases gradually from deep to shallow. In order to reveal the effect of GPS data for the Wenchuan earthquake, we adopt a 3D complex fault model and a large amount of GPS data to obtain the slip distribution of this earthquake. Based on the research results about the three-dimensional fault model, aftershock distribution, and surface rupture investigation, the 3D complex fault model is established. The south section of BCF adopts the model with dip angle gradually increasing from deep to shallow. The main

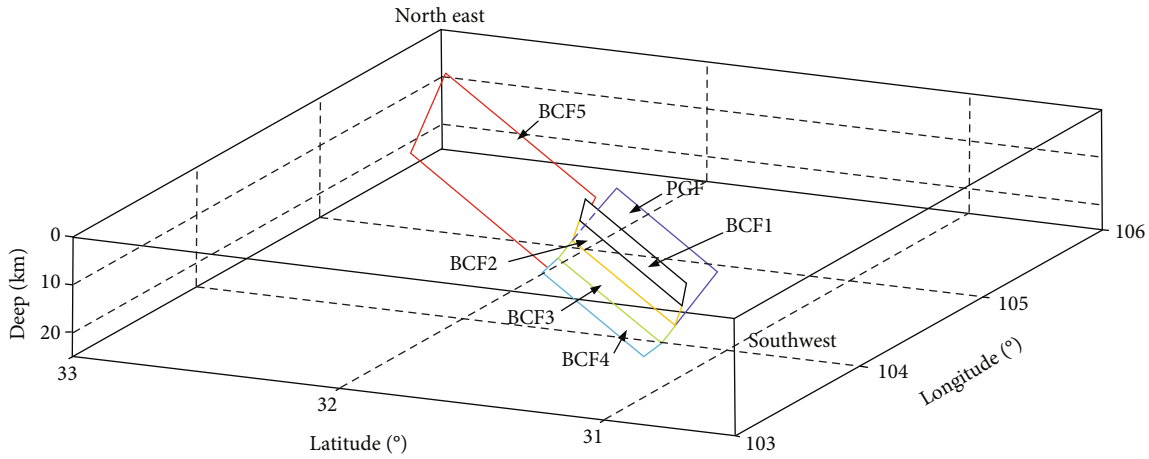

Figure 1: The 3D complex fault model of the Wenchuan earthquake.

purpose of this study is to research whether GPS data can distinguish slip on a complex fault.

2. Fault Rupture Model

According to the results of [1, 3] and Hubbard et al. (2009, 2010), the seismogenic fault of the Wenchuan earthquake has obvious segmentation characteristics. The source ruptured towards the northeast, and the dip angle gradually increased. In the southern part of the fault, the dip angle gradually increases from deep to shallow. On the basis of this research, a 3D complex fault model is established [17]. Here, the 3D fault model is adopted (Figure 1). The model contains the Beichuan fault (BCF) and the Pengguan fault (PGF). The southern part of the BCF fault has four segments: BCF1, BCF2, BCF3, and BCF4 with the dip angles of 65°, 50°, 33°, and 20°, respectively. The northern part of the BCF fault is BCF5 with a dip angle of 60°. The dip angle of PGF is 33°. The sizes of BCF1, BCF2, BCF3, and BCF4 are 132 km × 6 km, 132 km × 6 km, 132 km × 12 km, and 132 km × 15 km, respectively. The sizes of BCF5 and PGF are 180 km × 30 km and 132 km × 18 km, respectively. The size of the subfault is 5 km × 3 km. The number of subfaults of BCF1, BCF2, BCF3, BCF4, BCF5, and PGF is 52, 52, 104, 130, 360, and 156, respectively.

3. Data

After the Wenchuan earthquake, the Working Group of the Crustal Motion Observation Network of China Project (WGCMONCP) obtained detailed GPS observation data [24]. GPS data represents the static displacement of the ground surface and does not involve time information. Considering the distribution of stations and the quality of records, stations distributed on both sides of the fault with good record quality are selected. The horizontal coseismic displacements recorded by 120 stations are selected as inversion data, and the location of these stations is shown in Figure 2. The location information of these stations can be obtained from the WGCMONCP [24]. The horizontal displacement observed at the H035 station near Beichuan is the largest, with the East-West displacement of 2.379 m and the North-South displacement of 0.481 m. The station is about 2 km away from the surface rupture. At the southern end of the surface rupture, the East-West displacement of the H049 station is 1.276 m, and the North-South displacement is 0.801 m. At the north end of the surface rupture, the East-West displacement of the H010 station is 0.415 m, and the North-South displacement is 1.005 m. With the increase of fault distance, the observed permanent displacement decreases rapidly. The location of station 2037 is located in the footwall, with fault distance of 100 km. The observed East-West displacement is 0.115 m, and the North-South displacement is only 0.026 m. The H034 station, which is located in the hanging wall with a fault distance of about 90 km, has an East-West displacement of 0.209 m and a north-south displacement of only 0.055 m.

From the distribution of these stations, there is a certain amount of GPS stations in the area close to the seismogenic fault. There are QLAI, H060, 2049, Z246, PIXI, H050, H049, and H044 in the south section of the Beichuan fault and PGF. There are the H035 and Z122 stations near Beichuan, 2020 and H032 stations near Nanba, and the H010 station near the north end of the fault. The GPS observation values of these stations are large, and in the inversion, the observation GPS data is not normalized. So, the observation GPS data with large values are very important to constrain the slip distribution on the fault plane.

4. Method

The nonnegative least-square inversion method is utilized for this inversion [25]. The fault is divided into the subfaults with size 5 km × 3 km according to the result of Hartzell et al. [9]. The slip of these subfaults is the matrix x. The observed data of stations is matrix b. The calculation of Green's function of the GPS station is based on the program of psgrn and pscmp of Wang et al. [26]. A 1D crustal velocity model (Table 1) is selected according to Hartzell et al. [9]. Matrix A is the green function. The inversion function is as follows.

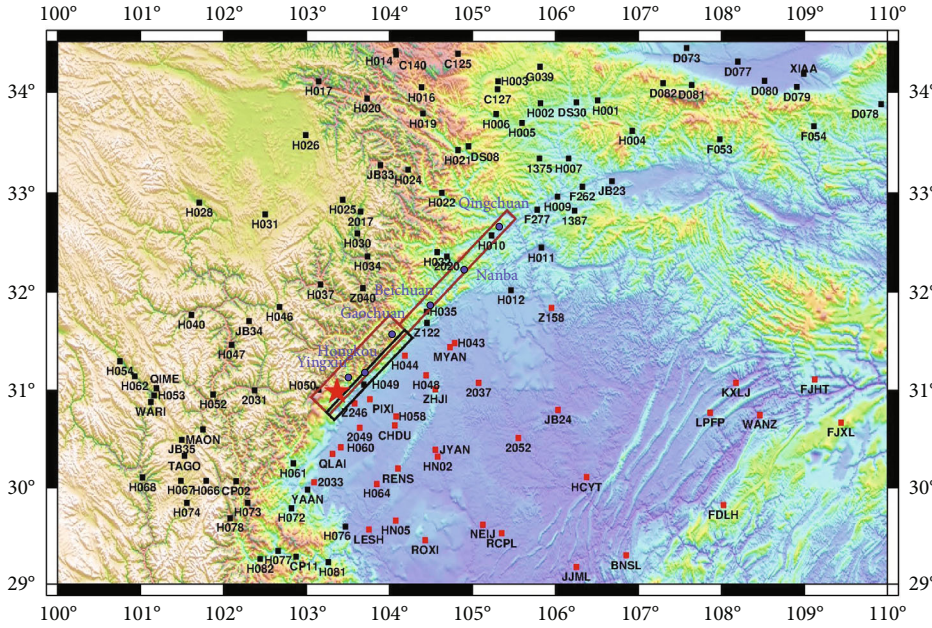

Figure 2: The position of 120 horizontal GPS observation stations; red and black squares indicate the footwall and hanging wall stations, respectively. The rectangle box is the projection of the fault, and the pentagram is the epicenter. The blue circles indicate towns.

Table 1: The structural mode.

Sichuan (footwall)	V_p (km/s)	V_s (km/s)	Density (g/ml)	Thickness (km)	Q_p	Q_s
	4.8	2.7	2.2	6	200	100
	6.0	3.4	2.4	4	600	300
	6.2	3.5	2.6	15	600	300
	6.6	3.8	2.8	15	600	300
	8.08	4.47	3.37	—	800	400
Tibet(hanging wall)	6.0	3.4	2.4	10	600	300
	6.2	3.5	2.6	15	600	300
	5.9	3.1	2.6	20	600	300
	6.6	3.8	2.8	10	600	300
	8.08	4.47	3.37	—	800	400

$$\begin{bmatrix} A \\ \lambda_1 M \\ \lambda_2 S \end{bmatrix} [x] \cong \begin{bmatrix} b \\ 0 \\ 0 \end{bmatrix}. \quad (1)$$

The inversion is stabilized by appending smoothing, S, and moment minimization, M, constraints to the least-square problem (Hartzell et al. [9]). The matrix of M is a unit diagonal matrix utilized to minimize moments by letting $x_i = 0$. The smoothing constraint matrix of S is utilized to minimize differences of slip between adjacent subfaults. The weights λ_1 and λ_2 can control the trade-off between satisfying these constraints and fitting the data. The values of λ_1 and λ_2 can be obtained by trial and error.

Compared with seismic data inversion, GPS data inversion is relatively simple, because it does not involve the time process of rupture. The subfault contains only one time window, and it does not matter with source time function. For calculating Green's function, the displacement at the station can be obtained by assuming that the subfault has slip 1 m along the strike and dip direction. The observed GPS data has certain error, about 1-5 mm [24]. The observed values of the stations far away from the fault are small and may have great uncertainty (Shen et al. [13], Hartzell et al. [9]). The error of observed GPS data is caused by the observation instrument or the observation method itself [24]. So, the records with small observed values may have greater uncertainty. In the inversion, the data is not normalized; the records with small observed values occupy a small weight in inversion. In the inversion, the data is not normalized, so the records with small observed values and greater uncertainty occupy a very small weight. In the inversion, the number of equations is 240, and the number of parameters is 1708. The number of equations is less than the number of parameters. In inversion, it is necessary to apply limiting conditions to obtain a stable solution. The limiting conditions is the matrix of M and S in formula (1).

5. Result

5.1. Observed and Synthetic GPS Data. Form the comparison between observed and synthetic GPS data (Figure 3), the large amplitude of these stations near the fault are well explained, such as H050, Z246, 2049, PIXI, H049, H044, Z122, H035, H032, 2020, H010, H011, and H012. On the other hand, the observed data for the stations with large fault distance are not well simulated. These stations with small fault distance are important to recover the slip distribution.

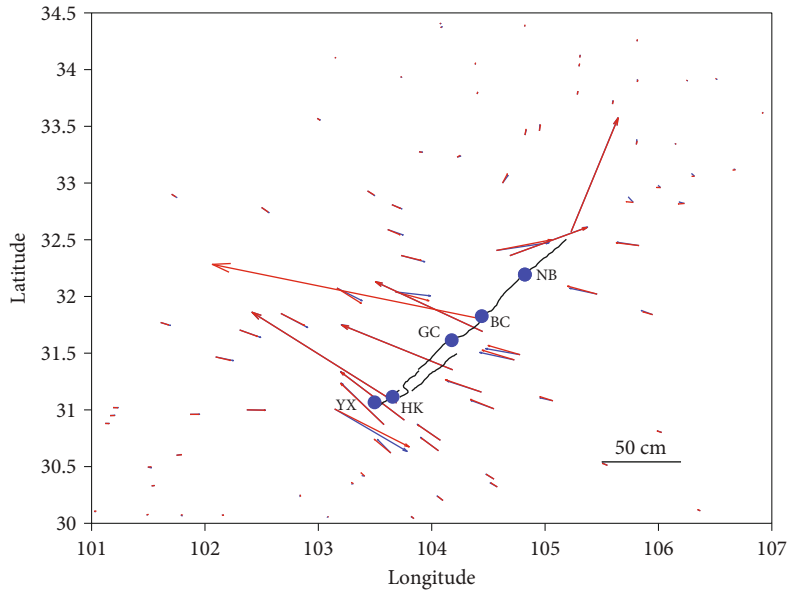

Figure 3: Comparison between observed GPS data (blue curves) and synthetic data (red curves).

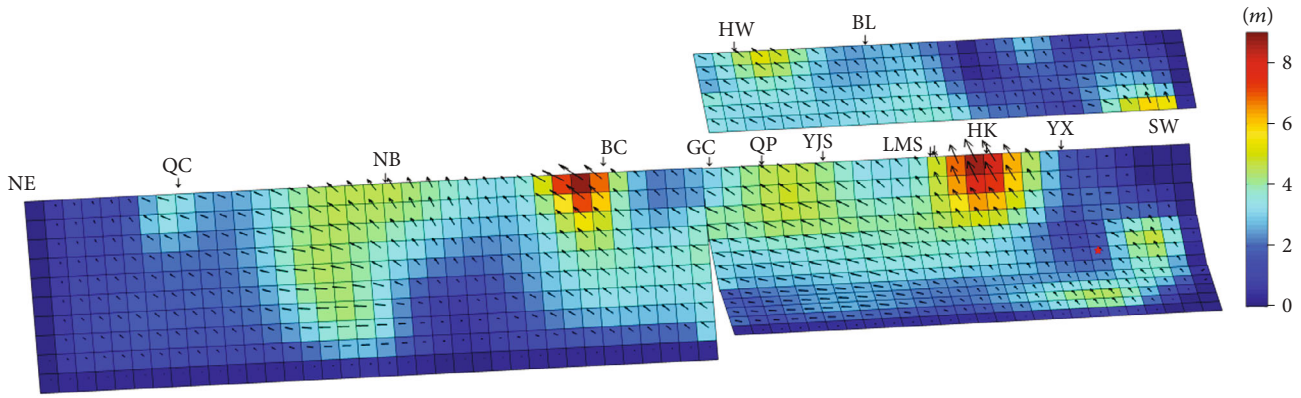

Figure 4: The slip distribution of the 3D model of Wenchuan earthquake based on inversion of GPS data. The characters are the towns. BL: Bailu; HW: Hanwang; YX: Yingxiu; HK: Hongkou; LMS: Longmenshan; YJS: Yuejiashan; QP: Qingping; GC: Gaochuan; BC: Beichuan; NB: Nanba; QC: Qingchuan.

Table 2: The inversion result.

PGF Slip/m	Moment (10^{21} N·m)	BCF1-4 Slip (m)	Moment (10^{21} N·m)	BCF5 Slip (m)	Moment (10^{21} N·m)	Moment (10^{21} N·m)
5.8	0.159	8.6	0.423	8.8	0.377	0.959

5.2. Slip Distribution. The result are shown in Figure 4 and Table 2. The seismic moment is 0.959×10^{21} N · M. According to the consistency between the magnitude and direction of the result, the synthetic records are in good agreement with the observed horizontal deformation vectors. The slip is mainly distributed in the shallow part of the fault. On the Beichuan fault, the slip is concentrated near the surface point of Hongkou, Qingping, Beichuan, and Nanba, which have large coseismic displacement. The slip on PGF is much smaller, which is distributed at the bottom of the southern end of the fault and the area from Bailu to Hanwang.

The maximum slip of the south section of Beichuan fault is 8.6 m, which is located near the surface of Hongkou. The seismic moment is 0.423×10^{21} N · M, accounting for 44% of the total seismic moment. The near surface area of Hongkou is dominated by thrust, and the area near Qingping is also dominated by thrust dislocation. The maximum slip of PGF is 5.8 m, and the released seismic moment is 0.159×10^{21} N · M, accounting for 17% of the total seismic moment. The slip on the fault is dominated by thrust. The maximum slip on BCF5 is 8.8 m, and the released seismic moment is 0.377×10^{21} N · M, accounting for 39% of the total seismic

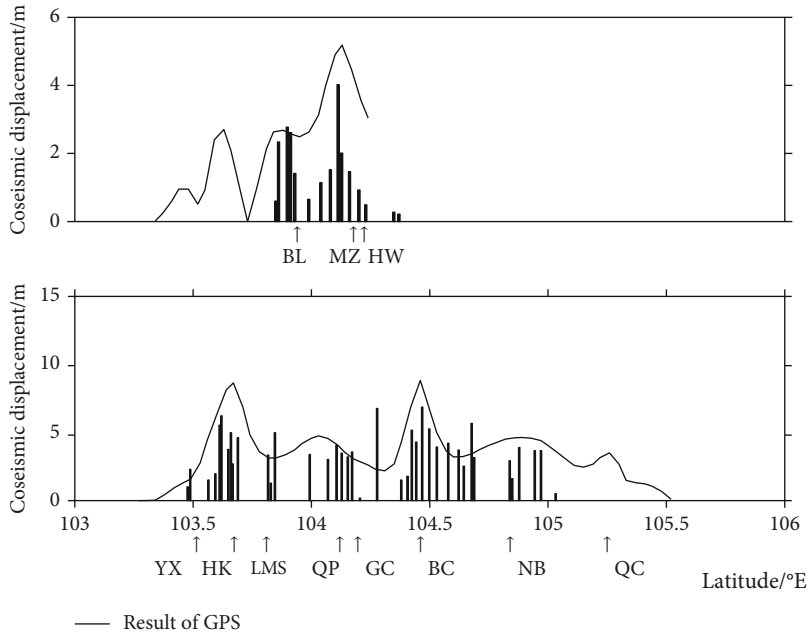

Figure 5: Comparison between observed coseismic displacement (vertical lines) and the slip of the subfaults near the surface area according to the inversion result (black curves). The top is the PGF, the bottom is the BCF.

moment. Near the surface of Beichuan and Nanba, there are strike and thrust dislocation.

In general, the slip is mainly distributed at a depth of above 15 km. In the south section of the Beichuan fault, the slip is concentrated from the Yingxiu to Longmenshan and from the Yuejiashan to Qingping areas with high dip angles. On BCF5, the slip is concentrated near the surface of Beichuan. In the area of Nanba and the north of Nanba, the dislocations are distributed in the range of about 35 km from the near surface of Nanba to the north side of Nanba. The slip under Nanba is strike slip. On the PGF, the slip is concentrated in the area near the surface of Hanwang and the area under the Bailu. The slip is thrust near Hanwang. The slip in the deep area is very small.

5.3. Coseismic Displacement and Slip Near Surface Area. The comparison between coseismic displacement and slip of the subfaults near the surface area is shown in Figure 5. The comparison of results shows that for the points where coseismic displacements are observed, the slip of the subfaults near the surface area is in good agreement with the observed coseismic displacement. For PGF, there is slip near the surface in the southern part. But the observed data is not obtained. Near BL, these two data are equal. Near the MZ (Mianzhu), the inversion data is larger than the observed data. On BCF, the amplitude of the inversion data is almost the same as that of the observed value. Near YX, BC, and NB, the inversion data is a little bigger than the coseismic displacement.

The inversion result shows that the slip near surface subfaults is almost the same as the observed value. For the inversion conducted by the seismic record, the result is worse than the GPS data.

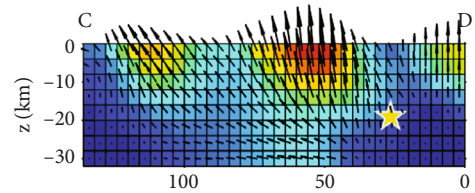

Figure 6: The coseismic slip from joint inversion of InSAR and GPS data of southern segment of BCF (Feng et al. [7]).

5.4. Comparison with Other Research Results. From the results of other researches on the utilized GPS data [6, 7, 9, 13], the locations of the rupture and slip type in the fault are similar. Although the fault models and number of GPS data are different, the rupture is mainly occurred near the start rupture point, Yingxiu, Yuejiashan, Beichuan, and Nanba areas. The slip in the PGF is smaller than BCF. But the value of the slip and size of the slip area are different.

Feng et al. [7] obtained the coseismic fault slip from the joint inversion of InSAR and GPS data. The fault model of BCF contained three segments with different dip angles. The southern segment of BCF has a dip angle of 47° (Figure 6). In this paper, the fault of the southern segment of BCF has different dip angles from deep to shallow with 20°, 33°, 50°, and 65°. Both results showed that the slip is mainly distributed near Hongkou and Qingping areas. The slip pattern near Hongkou is the dip slip with maximum slip value. The slip near Qingping is mainly the dip slip with a small amount of strike slip. Feng et al. [7] obtained that the slip near the south end of BCF in Figure 6 has a certain amount of slip. It is worth noting that the results in this paper showed that there is no sliding in this region. There is certain sliding at the lower side of the south section of

PGF fault with the same slip pattern. GPS data do not easily distinguish the slip on two faults that are very close in space.

It is noteworthy that the change trend of the slip near surface subfaults is coincident with the observed coseismic displacement for various researches. The GPS data is useful to determine the slip in the shallow part.

6. Discussion

In order to demonstrate the strengths and limitations of geodetic in the inversion of rupture process, the rupture history of the Wenchuan earthquake is obtained by a large number of observation records. From the comparison between observed and synthetic GPS data, the coincidence degree of near fault stations with a large amplitude is better than that of stations with small amplitude faraway form the fault. The amplitude of observation record decreases sharply with the increase of distance. Therefore, it is very important to select stations close to the fault with large amplitude for limiting the inversion result. The observed values have the range 2-5 mm uncertainties [13]. So, the stations far away from the fault have larger uncertainties. In the inversion, it is not necessary to normalize the observation records. The smaller values with larger uncertainty have less weight in the inversion.

In our inversion, the strengths and limitations of geodetic data are obvious. The inversion is very easy to achieve, because it includes the simple point measurement data with no time dimension. Because the observations represent real ground motion, the observed data can accurately limit the location of the slip.

The results of GPS data can only reflect the slip in the shallow part and cannot reveal the fracture in the deep part. We only take the slip values of some fault areas and synthesize GPS data through the forward modeling method, so as to analyze the contribution of slip in different areas to the synthetic records. The reliability analysis of the results shows that the slip of the shallow part on the fault plane is the main contribution to the synthetic record of the stations near the fault, such as H035, H049, and H010. The contribution of the deep regional slip to synthetic records is much smaller. From the result of geodetic inversion, the slip is mainly concentrated in the shallow areas. Then, the GPS data are crucial for controlling the slip on the shallow part but are insensitive to deeper faulting.

7. Conclusion

For the purpose of reproducing the slip distribution of the Wenchuan earthquake, the GPS data and 3D fault model are adopted. The results show that the Beichuan fault is mainly the rupture plane for this earthquake. The maximum slip is about 9.0 m. The Beichuan fault has five large slip areas (asperity). One is located near the start rupture point. The two asperities near Hongkou and Beichuan have large slip values. Near Yuejiashan and Nanba are the rest asperities. In total, the slip changes from thrust to thrust and strike slip from south to north. Although the fault models and GPS data are different for the researches, the inversion results of GPS data are similar. The slip is mainly concentrated near the surface of Beichuan fault, near Hongkou, Qingping, Beichuan, and Nanba area.

It can be seen from the comparison between the slip near surface area and coseismic displacement that for the points where coseismic displacements are observed, the slip of the subfaults near surface area are in good agreement with these observed coseismic displacements. It shows that the inversion result of GPS data is relatively stable and the data is very important for constraining the slip dislocation in the fault plane.

Data Availability

The data used to support the research in this study are available from the corresponding author upon request.

Conflicts of Interest

The article does not involve conflict of interest.

Acknowledgments

This research is supported by the Natural Science Foundation of Jiangsu Province (grant nos. BK20210950 and BK20181061), Huaian Natural Science Research Plan (HAB202060), and Open Fund for Jiangsu Engineering Laboratory of Structure Assembly Technology on Urban and Rural Residence, Huaiyin Institute of Technology (JSZP201903).

References

[1] X. Xi-Wei, W. Xue-Ze, Y. Jian-Qing et al., "The Ms8.0 Wenchuan earthquake surface rupture and its seismogenic structure," *Seismology and Geology*, vol. 30, no. 3, pp. 597–629, 2008.

[2] C. Xu, Y. Liu, Y. Wen, and R. Wang, "Coseismic slip distribution of the 2008 Mw 7.9 Wenchuan earthquake from joint inversion of GPS and InSAR data," *Bulletin of the Seismological Society of America*, vol. 100, no. 5B, pp. 2736–2749, 2010.

[3] X. Xu, X. Wen, G. Yu et al., "Coseismic reverse- and oblique-slip surface faulting generated by the 2008 Mw 7.9 Wenchuan earthquake, China," *Geology*, vol. 37, no. 6, pp. 515–518, 2009.

[4] X. W. Xu, G. H. Chen, G. H. Yu et al., "Reevaluation of surface rupture parameters of the 5·12 Wenchuan earthquake and its tectonic implication for Tibetan uplift," *Chinese Journal of Geophysics*, vol. 53, no. 10, pp. 2321–2336, 2010.

[5] G. H. Chen, X. W. Xu, G. H. Yu et al., "Co-seismic slip and slip partitioning of multi-faults during the Ms8. 0 2008 Wenchuan earthquake," *Chinese Journal of Geophysics*, vol. 52, no. 5, pp. 1384–1394, 2009.

[6] Q. Chen, Y. Yang, R. Luo, G. Liu, and K. Zhang, "Deep coseismic slip of the 2008 Wenchuan earthquake inferred from joint inversion of fault stress changes and GPS surface displacements," *Journal of Geodynamics*, vol. 87, pp. 1–12, 2015.

[7] G. Feng, E. A. Hetland, X. Ding, Z. Li, and L. Zhang, "Coseismic fault slip of the 2008 Mw 7.9 Wenchuan earthquake estimated from InSAR and GPS measurements," *Geophysical Research Letters*, vol. 37, no. 1, pp. 73–78, 2010.

[8] E. J. Fielding, A. Sladen, Z. Li, J. P. Avouac, R. Bürgmann, and I. Ryder, "Kinematic fault slip evolution source models of the

2008 M7.9 Wenchuan earthquake in China from SAR interferometry, GPS and teleseismic analysis and implications for Longmen Shan tectonics," *Geophysical Journal International*, vol. 194, no. 2, pp. 1138–1166, 2013.

[9] S. Hartzell, C. Mendoza, L. Ramirez-Guzman, Y. Zeng, and W. Mooney, "Rupture history of the 2008 Mw 7.9 Wenchuan, China, earthquake: evaluation of separate and joint inversions of geodetic, teleseismic, and strong-motion data," *Bulletin of the Seismological Society of America*, vol. 103, no. 1, pp. 353–370, 2013.

[10] K. Koketsu, K. Hikima, H. Miyake, T. Maruyama, and Z. Wang, *Source Process and Ground Motions of the 2008 Wenchuan, China, Earthquake*, Agu Fall Meeting Abstracts, 2008.

[11] T. Nakamura, S. Tsuboi, Y. Kaneda, and Y. Yamanaka, "Rupture process of the 2008 Wenchuan, China earthquake inferred from teleseismic waveform inversion and forward modeling of broadband seismic waves," *Tectonophysics*, vol. 491, no. 1–4, pp. 72–84, 2010.

[12] T. Nakamura, S. Tsuboi, Y. Kaneda, and Y. Yamanaka, "Rupture of deep faults in the 2008 Wenchuan earthquake and uplift of the Longmen Shan," *Nature Geoscience*, vol. 4, no. 9, pp. 634–640, 2011.

[13] Z. K. Shen, J. Sun, P. Zhang et al., "Slip maxima at fault junctions and rupturing of barriers during the 2008 Wenchuan earthquake," *Nature Geoscience*, vol. 2, no. 10, pp. 718–724, 2009.

[14] X. Tong, D. T. Sandwell, and Y. Fialko, "Coseismic slip model of the 2008 Wenchuan earthquake derived from joint inversion of interferometric synthetic aperture radar, GPS, and field data," *Journal of Geophysical Research: Solid Earth*, vol. 115, no. B4, pp. 150–150, 2010.

[15] W. Wei-Min, Z. Lian-Feng, L. Juan, and Y. Zhen-Xing, "Rupture process of the Ms 8.0 Wenchuan earthquake of Sichuan, China," *Chinese Journal of Geophysics*, vol. 51, no. 5, pp. 1403–1410, 2008.

[16] D. Y. Yin, *Research on the Wenchuan earthquake rupture process of joint inversion and high-frequency radiation [PhD Thesis]*, Institute of Engineering Mechanics, China Earthquake Administration, 2017.

[17] D. Yin, Q. Liu, and J. Wu, "Estimation of the Wenchuan earthquake rupture sequence utilizing teleseismic records and Coseismic displacements," *Advance in civil engineering*, vol. 2018, article 2147683, pp. 1–13, 2018.

[18] J. Hubbard and J H. Shaw, "Uplift of the Longmen Shan and Tibetan plateau, and the 2008 Wenchuan $(M = 7.9)$ earthquake," *Nature*, vol. 458, no. 7235, p. 194, 2019.

[19] J. Hubbard, J H. Shaw, and Y. Klinger, "Structural Setting of the, Mw 7.9 Wenchuan, China, Earthquake," *Bulletin of the Seismological Society of America, 2010*, vol. 100, no. 5B, pp. 2713–2735, 2008.

[20] D. Y. Yin, Y. Dong, Q. F. Liu, Y. Chen, and Y. She, "Estimation of high-frequency seismic wave radiation on fault plane of 2008 Wenchuan earthquake based on improved empirical Green's function," *Natural Hazards*, vol. 104, no. 1, pp. 397–412, 2020.

[21] D. Y. Yin, Y. Dong, Q. F. Liu et al., "Estimating the areas of high-frequency wave radiation on the fault plane of the 2008 Mw 7.9 Wenchuan, China, earthquake by envelope inversion," *Bulletin of the Seismological Society of America*, vol. 111, no. 2, pp. 975–988, 2021.

[22] Y. Zhang, W. P. Feng, L. S. Xu, C. H. Zhou, and Y. T. Chen, "The rupture process of the great Wenchuan earthquake," *Science China Earthquake Sciences*, vol. 38, no. 10, pp. 1186–1194, 2008.

[23] C. P. Zhao, Z. L. Chen, L. Q. Zhou, Z. X. Li, and Y. Kang, "Rupture process of the 8.0 Wenchuan earthquake of Sichuan, China: the segmentation feature," *Chinese Science Bulletin*, vol. 55, no. 3, pp. 284–292, 2010.

[24] Working Group of the Crustal Motion Observation Network of China Project (WGCMONCP), "Coseismic displacement field of the 2008 M_s 8.0 Wenchuan earthquake determined by GPS," *Science China Earth Sciences*, vol. 38, pp. 1195–1206, 2008.

[25] S. H. Hartzell and T. H. Heaton, "Inversion of strong ground motion and teleseismic waveform data for the fault rupture history of the 1979 Imperial Valley, California, earthquake," *Bulletin of the Seismological Society of America*, vol. 73, no. 6A, pp. 1553–1583, 1983.

[26] R. Wang, F. Lorenzo-Martín, and F. Roth, "PSGRN/PSCMP–a new code for calculating co- and post-seismic deformation, geoid and gravity changes based on the viscoelastic-gravitational dislocation theory," *Computers & Geosciences*, vol. 32, no. 4, pp. 527–541, 2006.